Impact of drought on ecosytem functionning and water-use strategy of a seed potato crop (*Solanum tuberosum* L.) : a three years study (2010, 2014, 2018)

Quentin BEAUCLAIRE, Louis GOURLEZ DE LA MOTTE, Bernard HEINESCH, Anne DE LIGNE, Bernard LONGDOZ

Biosystem Dynamics and Exchanges (BioDynE), TERRA Teaching and Research Center, Gembloux Agro-Bio Tech, ULiège Université

Contact : q.beauclaire@uliege.be

1. Context and objectives

- Impact of climate change on the supply of agrosystems in ecosystem services
- Impact of drought duration and frequency on carbon assimilation

---

- To infer from gas exchange measurements (EC) at the ecosystem level its water-use adaptation during drying-up events
- To evaluate wether potato photosynthesis during drought is impacted by stomatal or non-stomatal limitations (biochemical/mesophyll)

2. Site

ICOS Lonzée Station (BE-Lon)

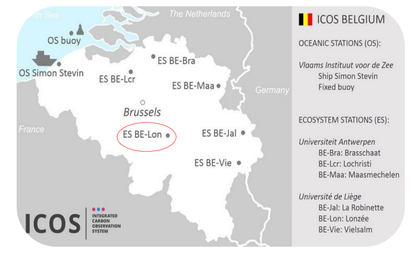

- Temperate climate (mean annual T and P: 10 °C, 800 mm)
- Land cultivated for more than 80 years
- Four-year rotation typical of central Belgium and including seed potaoes
- Soil type : loamy soil with plowed horizon over the 30 first cms

2. Methodology

- Underlying theory : Reduction of carbon assimilation during drought due to decrease in stomatal (g_s)/mesophyll (g_m) conductance and/or a reduction in Rubisco (V_{cmax})/RuBP activity (J_{max}). Under high irradiance, the Calvin cycle becomes limited by Rubisco. Mesophyll conductance is assumed to be infinite, making the chloroplastic [CO_2] ≌ leaf internal [CO_2] (fig. 1).
- g_s determined by inverting the Penman equation (Penman, 1948) (Eq. 1.1) at the canopy scale (G_c). G_a calculated using Thom (1972) (Eq. 1.2).
- Use of the Medlyn model (Medlyn et al., 2011) to quantify canopy sensitivity to photosynthesis (G_1) by daily regressions (Eq. 2). G_1 is inversely proportional to intrinsic water use efficiency (iWUE) (Medlyn et al., 2011).
- Apparent V_{cmax} calculation based on Arneth et al. (2002) (Eq. 3.1) . Γ^* is CO_2 compensation point and K_m is the Michaelis-Menten coefficient for Rubisco kinetics. C_i calculation based on a fickian law (Eq. 3.2). Decrease in V_{cmax} can be either due to decrease in g_m or real biochemical alteration.
- By setting apparent V_{cmax} and G_1 to their unstressed values, and by calculating GPP based on these conditions (GPP_{mod}), the comparison of GPP_{mod} to GPP_{dat} (measured) by the ratio GPP_{mod}/GPP_{data} provides an index for water stress impact on GPP modelling (Zhou et al., 2013).
- Soil water availability determined by relative extractable water (REW) along the root zone, representing the fraction of available water to plant uptake (4). θ_{wp} = wilting point and θ_{fc} = field capacity. Maximum daily root depth modelled based on Hartmann et al. (2017).
- REddyProc package for post-processing EC data treatments (Wutzler et al., 2018). GPP, G_c and V_{cmax} normalized by green leaf area index (LAI) under saturated irradiance (PPFD > 1200 µmol.m^{-2}.s^{-1}) to remove the impact of both irradiance and phenology. Daily LAI determined based on measurements and fitting to growing degree days (GDD) by a sigmoidal response (Su et al., 2015). Data selected as follows : 48h after the last rainfall, active vegetation (LAI>2) and no gapfilling.

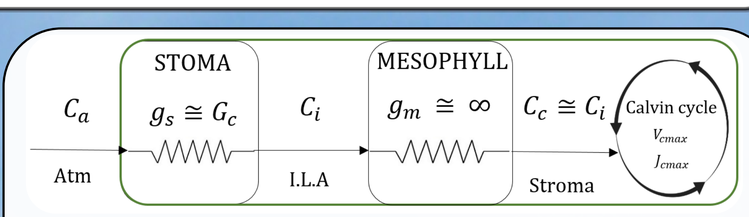

Figure 1 : Representation of simplified CO_2 pathways in the cell and the corresponding resistances. C_a corresponds to atmospheric [CO_2] C_i to leaf intracellular [CO_2,] C_c to chloroplastic [CO_2]. g_s is the stomatal conductance, g_m the mesophyll conductance, G_c the canopy conductance. ILA means intracellular leaf airspace. V_{cmax} and J_{max} denote respectively the maximum Rubisco carboxylation rate and the maximum electron transport rate.

(1.1) $$g_s \cong G_c = \frac{G_a \gamma LE}{\Delta(R_n - G) + \rho c_p G_a VPD - (\Delta + \gamma)LE}$$ (1.2) $$G_a = \frac{u_*^2}{u} + \frac{1}{6u_*^{-0.667}}$$

(2) $$g_s \cong G_c = 1.6\left(1 + \frac{G_1}{\sqrt{VPD}}\right)\frac{GPP}{C_s}$$

(3.1) $$V_{cmax} = \frac{GPP(C_i + K_m)}{C_i - \Gamma^*}$$ (3.2) $$C_i = C_a - \frac{GPP}{G_c}$$

(4) $$REW = \frac{\sum_{surf}^{root\ depth} \theta - \theta_{wp}}{\sum_{surf}^{root\ depth} \theta_{fc} - \theta_{wp}}$$

3. Results

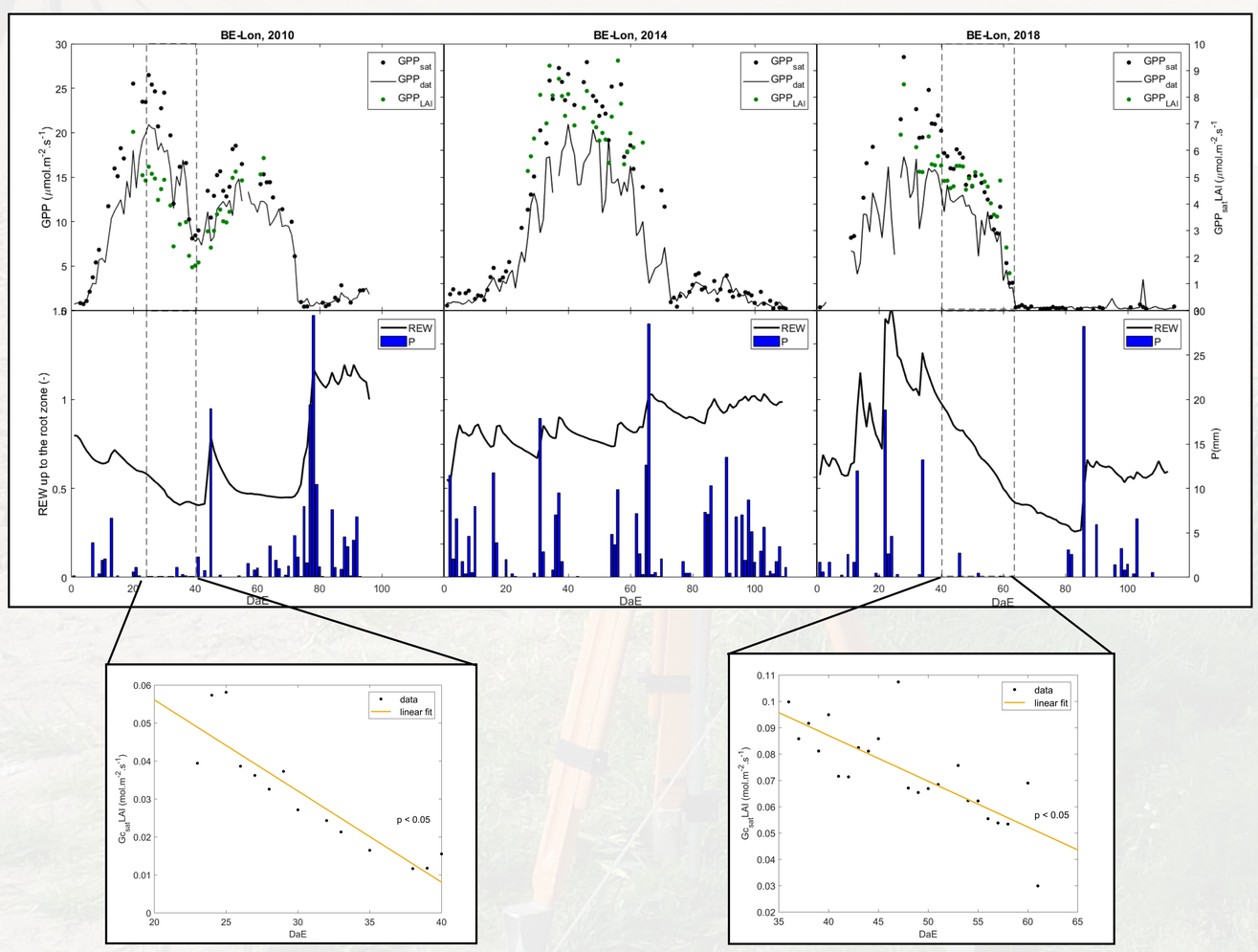

Figure 2: GPP_{dat} (measured photosynthesis), GPP_{sat} (saturated photosynthesis) and GPP_{LAI} (normalized saturated photosynthesis per leaf m^2) fluxes (mean per day) during the years 2010, 2014 and 2018 for the graphes in the first row. In the second row, REW and precipitation are shown for the three years. Dashed rectangles highlight GPP_{LAI} anomalies periods. Zoom-in graphs represent the evolution of saturated G_c normalized by LAI during drying-up episodes. DaE refers to days after emergence .

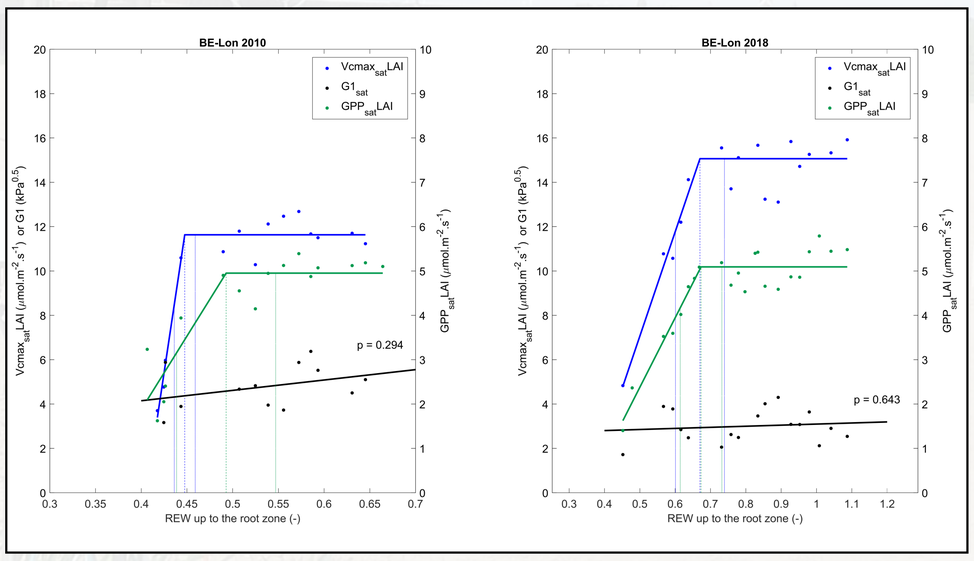

Figure 3: Evolution of GPP_{LAI}, G_1 and V_{cmax} regarding to REW in 2010 and 2018 during GPP anomaly periods. Segmented linear regression (method not shown) was used to determined the presence of a REW threshold (breakpoint) for GPP_{LAI} and V_{cmax} .G_1 was fit to REW using a linear regression. p-values represent the result of the F-test comparing the linear regression to a constant model.

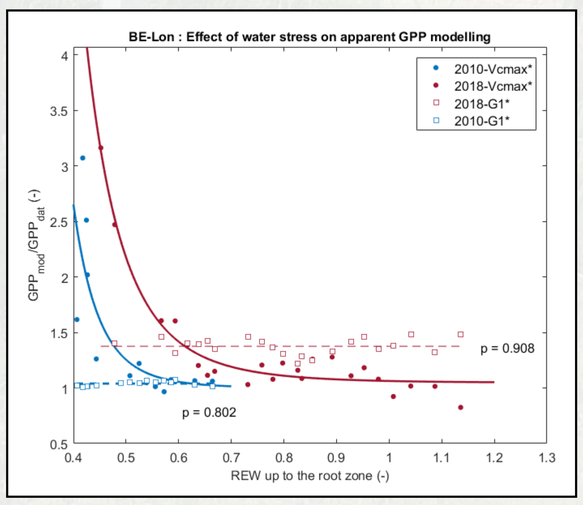

Figure 4 : Impact of setting V_{cmax} or G_1 to their unstressed values during drying up episodes (respectively V_{cmax}* and G_1*) on GPP potentially not impacted by REW during 2010 and 2018. Squares correspond to G_1* and circles to V_{cmax}*. V_{cmax}* dependance on REW was fitted using an expontial regression. G_1* dependance on REW was fitted using a linear regression. p-values represent the result of the F-test comparing the linear regression to a constant model.

4. Discussion

- GPP anomalies during both vegetative (DaE<40) and maturity (DaE>40) stages in 2010 and 2018. No significant anomaly in 2014 (fig.2). Concomitance with periods of decreasing REW.
- During these anomalies, G_c decreased, showing evidences of stomtal closure during drying-up events (fig. 2).
- No changes in carbon assimilation above the REW threshold (0.67 ± 0.6 in 2018 and 0.45 ± 0.03 in 2010 — defined as mild water stress). Decrease in saturated photosynthesis below REW thresholds (severe water stress), so did as apparent V_{cmax} (fig. 3).
- G_1 remained constant (no changes in iWUE during water stress). Decrease in V_{cmax} and GPP can be attributed to non-stomatal limitations on photosynthesis (including mesophyll diffusion or real biochemical alteration), which may become predominant under sever water stress (Manzoni et al., 2011).
- Differences in REW thresholds bewteen years could be explained by changes in soil water probes, changes in potato species, soil spatial and temporal heterogeneity or uncertainty in θ_{fc} and θ_{wp} determination.
- By setting G_1 to its maximum value (ie. unstressed conditions), no impacts on GPP modelling, at the opposite of V_{cmax} (fig. 4). By impacting Vcmax, water stress led to a decrease in GPP about 3 times => need of accouting for REW impact on V_{cmax}, which is challenging in ecosystem modelling (Rodgers et al., 2017).

5. Conclusion and perspectives

- During drought (ie. REW<REWth), predominance of non-stomatal limitation on photosynthesis. We showed the neccesity of taking into account the effect of REW on V_{cmax} to avoid overestimations of the influence of stomatal closure on GPP computation (fig. 4).
- One explanation for the influence of non-stomatal limitations could come from changes in mesophyll conductance in several plant species (Keenan et al. 2009 ; Romero et al., 2017 ; Muir et al., 2014 ; Heerden et al., 2005), including potatoes (Obidiegwu et al., 2015).
- WUEi didn't increase during water stress, at the opposite of most assumptions predicting an increasing WUEi with drought (Zhou et al., 2013).
- Interpreting V_{cmax} and G_1 in a physiological context from EC data requires some precautions, especially with energy balance closure and storage flux computation (Knauer et al., 2018).

- Next issues consist in a proper modelling of g_m and a better understanding of underlying mechanisms in mesophyll regulation (Rodgers et al., 2017).